AIAA Aviation
16-20 June 2014, Atlanta, GA
7th AIAA Theoretical Fluid Mechanics Conference

2014

Airfoils Supporting Non-unique Transonic Solutions for Unsteady Viscous Flows

Kui Ou, *
Flight Sciences Department, Honda Aircraft Company, Greensboro, NC 27410
Antony Jameson,†
Aeronautics and Astronautics Department, Stanford University, Stanford, CA 94305
John C. Vassberg, ‡
Advanced Concepts Design Center, Boeing Commercial Airplanes, Long Beach, CA 90846

Non-unique numerical solutions of transonic flows have been found, first for potential flow equation, and later for Euler and RANS equations. The studies conducted so far have been mostly limited to steady state flow simulations. It is believed that unsteady simulations are needed to gain a better understanding of the evolution and stability of these flows. This paper re-examined a set of four recently designed symmetric airfoils that have been found to support non-unique solutions in steady transonic flows in a narrow band of transonic Mach numbers. Unsteady RANS solutions have been performed for these four airfoils in the transonic regime. Results indicate that all four airfoils exhibit unsteady non-unique transonic solutions. The unsteady non-unique solutions occur over a wider band of transonic Mach numbers than the steady non-unique solutions.

I. Introduction

Non-unique solutions of the transonic potential flow equation were discovered by Steinhoff and Jameson[1] (1981), who obtained lifting solutions for a symmetric Joukowski airfoil at zero angle of attack in a narrow range of Mach numbers in the neighborhood of Mach 0.85. This non-uniqueness could not be duplicated with the Euler equations and it was conjectured by Salas et al[2] (1983) that the non-uniqueness was a consequence of the isentropic flow approximation. Subsequently, however, Jameson[3] (1991) discovered several airfoils which supported non-unique solutions of the Euler equations in a narrow Mach band. These airfoils were lifting.

The question of non-unique transonic flows was re-examined by Hafez and Guo[4–6] (1999) who formed both lifting and non-lifting solutions for a 12 percent thick symmetric airfoil with parallel sides from 25 to 75 percent chord in a Mach range from 0.825 to 0.843. The question was further pursued in detail in a series of studies by Kuz'min and Ivanova[7–11] (2004,2006) who confirmed the results of Hafez and Guo, and also showed that airfoils with positive curvature everywhere could support non-unique solutions.

Recently, a set of four symmetrical airfoils was designed by Jameson, Vassberg, and Ou[15] (2011) which were found to support non-unique transonic solutions. The NU4 airfoil was the result of aggressive shape optimization to minimize drag of a 12 percent thick symmetrical airfoil. The JF1 airfoil is an extremely simple parallel sided airfoil. The JB1 airfoil is also parallel sided but has continuous curvature over the entire profile. The JC6 airfoil is convex and C_∞ continuous. The geometric shapes of these four airfoils are illustrated in Figure 1.

In non-lifting transonic flow these airfoils exhibit a transition from a solution with two supersonic zones on each surface below a certain critical Mach number to a situation with one supersonic zone on each surface above the critical Mach number. In the region of instability solutions with positive lift are found in which there is a single supersonic zone on the top surface and two supersonic zones on the lower surface. Solutions

*Flight Sciences Department, Honda Aircraft Company, AIAA Member
†Thomas V Jones Professor, Aeronautics and Astronautics Department, Stanford University, AIAA Fellow.
‡Boeing Technical Fellow, The Boeing Company, AIAA Fellow.

(a) NU4 airfoil (b) JF1 airfoil

(c) JC6 airfoil (d) JB1 airfoil

Figure 1. Geometric shapes of a set of 4 symmetric airfoils admitting non-unique transonic solutions.

with negative lift which are the mirror images of the solutions with positive lift. The $CL - \alpha$ plots of these airfoils exhibit three branches at zero angle of attack corresponding to a P-branch with positive lift, a Z-branch with zero lift, and a N-branch with negative lift. The results for NU4 and JB1 airfoils are shown in Figure 2. For further details of the study, please refer to Jameson, Vassberg, and Ou (2011).[15]

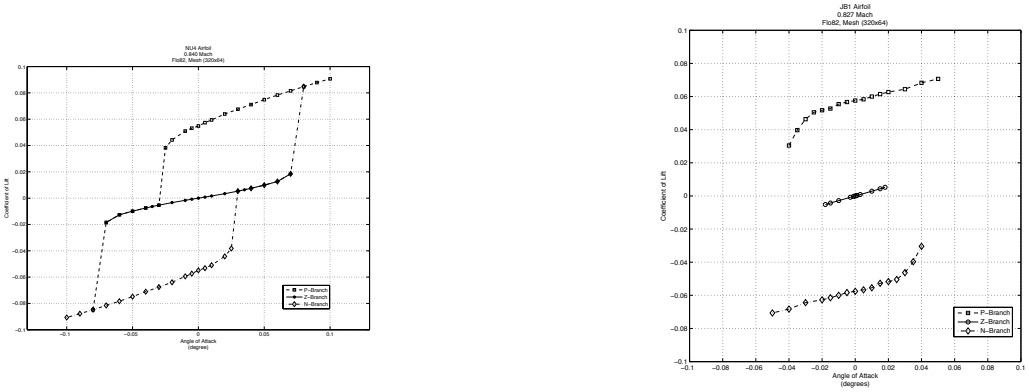

(a) NU4 airfoil (b) JB1 airfoil

Figure 2. $CL - \alpha$ plots of NU4 and JB1 airfoils. The overlapping of the P, Z, and N branches indicate non-uniqueness of flow solutions.

The reported non-unique solutions were obtained based on Euler equations. The Euler solver (FLO82)[13] uses a multigrid solution procedure, in combination with variable local time stepping and residual averaging. These procedures could potentially stabilize an otherwise unstable solution. There is a need to further verify the findings established by the Euler solutions using unsteady Navier-Stokes solutions.

II. Non-unique Transonic Solutions: Unsteady Viscous Flows

Flow simulations based on unsteady Navier-Stokes equations (UFLO103)[14] were performed in this paper. A Reynolds number of 6,000,000 has been used for all viscous flows. The airfoils all have C-topology meshes which contain 320 cells in the clockwise direction and 64 cells in the normal direction. The simulation procedure is as follows. For a given Mach number, an angle of attack is chosen, and the flow is computed until sufficient convergence is reached. The time-averaged lift coefficient is then recorded. This makes a data point in the Cl-alpha sweep curve. To collect the next data point, the previously converged flow solution was used as the initial condition. The time-accurate RANS simulations were performed for all four airfoils. The results for NU4 airfoil are discussed in further details below.

II.A. NU4 Airfoil - Geometry

NU4 airfoil is a consequence of a shape optimization study for symmetric airfoils in transonic flow,[12] in which an attempt was made to find a 12 percent thick airfoil with a shock free solution at Mach 0.84. The airfoil shape and the mesh near the airfoil are shown in Figure 3.

The $C_l - \alpha$ sweep shows that NU4 airfoil assumes unique solution at Mach 0.830. As the Mach number further increases, non-unique transonic solutions are observed, i.e. multiple C_l solutions are supported for a given Mach number and α. As the Mach number increases, the range of α that can support non-unique solutions widens. This is shown in Figure 4. In going from M.830 to M.837, the airfoil transitions from

(a) Airfoil shape (b) Mesh around the airfoil

Figure 3. NU4 airfoil shape and C-mesh around the airfoil.

admitting primarily Z-branch solution to admitting primarily P- and N-branch solutions. In the intermediate Mach numbers, all three branches exist. The Cp distributions corresponding to M.830 and M.837 are shown in Figure 5 and 6.

(a) M=.830 (b) M=.833 (c) M=.835 (d) M=.837

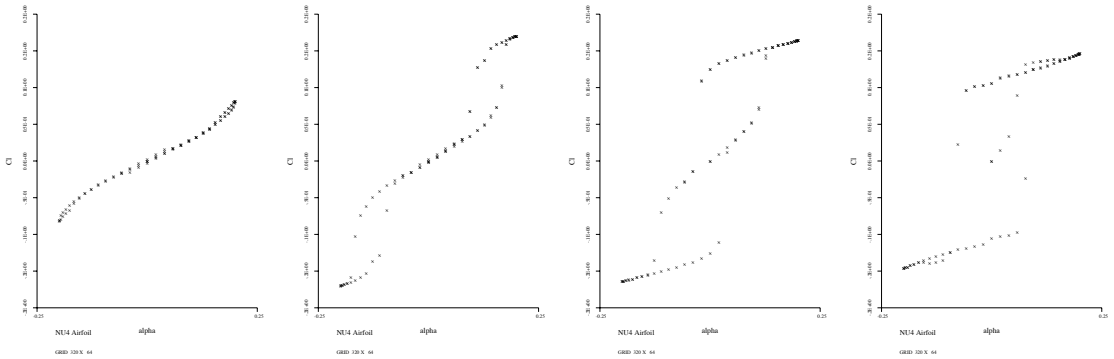

Figure 4. CL-α sweeps for NU4 airfoil at increasing Mach numbers.

(a) M=.830, $\alpha = 0°$ (b) M=.830, $\alpha = 0.20°$ (c) M=.830, $\alpha = 0°$

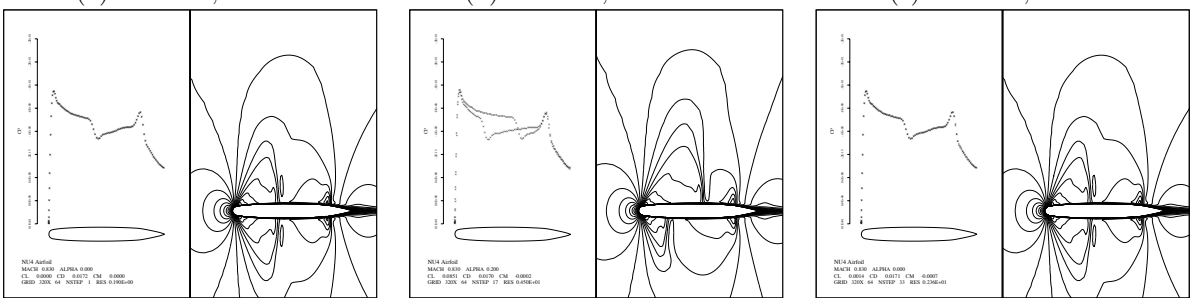

Figure 5. Cp distributions for NU4 airfoil at M.830. (a) Flow solution at zero angle of attack. (b) Flow solution at 0.2 degree angle of attack (c) Flow solution at zero angle of attack, following an initial perturbation to 0.2 degree angle of attack.

The opposite process occurs as the Mach number further increases. The range of α supporting non-unique flows becomes narrower. At sufficiently high Mach number, the transonic flows become unique again. The airfoil transitions from admitting primarily P- and N-branch solutions, to admitting only Z-branches solution. In the intermediate Mach numbers, all three branches exist.

It is found from studying the NU4 airfoil that non-unique transonic solutions can appear when multiple shocks are formed on the airfoil surface. If the shocks are far enough apart and do not interact with each other for a given range of disturbance, the solution remains unique, as is shown in the M=.830 case in Figure 5. On the other hand, if the shocks are closely spaced, and the perturbation is sufficient to cause the shocks to interact and coalesce, it can lead to non-unique flows, as is shown in the M=.837 case in Figure 6. The interaction of two shocks appears to be a non-linear process. It takes a certain condition for two shocks to coalesce into one single stronger shock, and a different condition for the same single shock to be separated back into two weaker shocks. As a result of the irreversible process, a same condition can be found that can admit a solution with a single strong shock, or a solution with two weak shocks. For example, at M=.841,

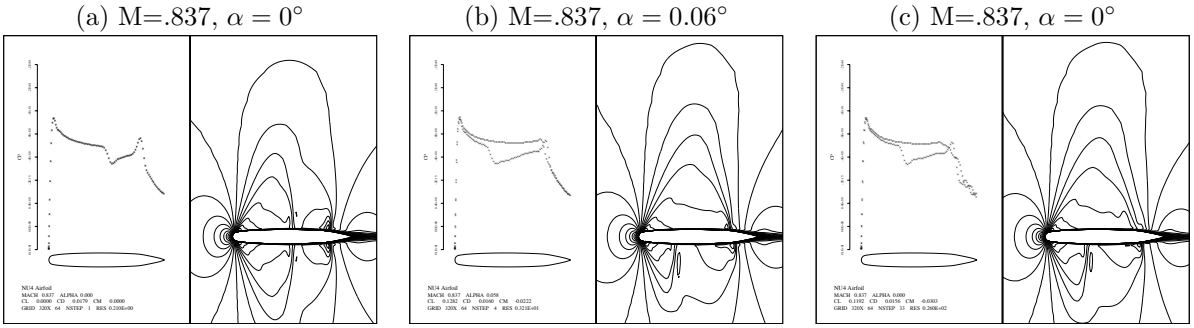

Figure 6. Cp distributions for NU4 airfoil at M.837. (a) Flow solution at zero angle of attack. (b) Flow solution at 0.06 degree angle of attack (c) Flow solution at zero angle of attack, following an initial perturbation to 0.06 degree angle of attack.

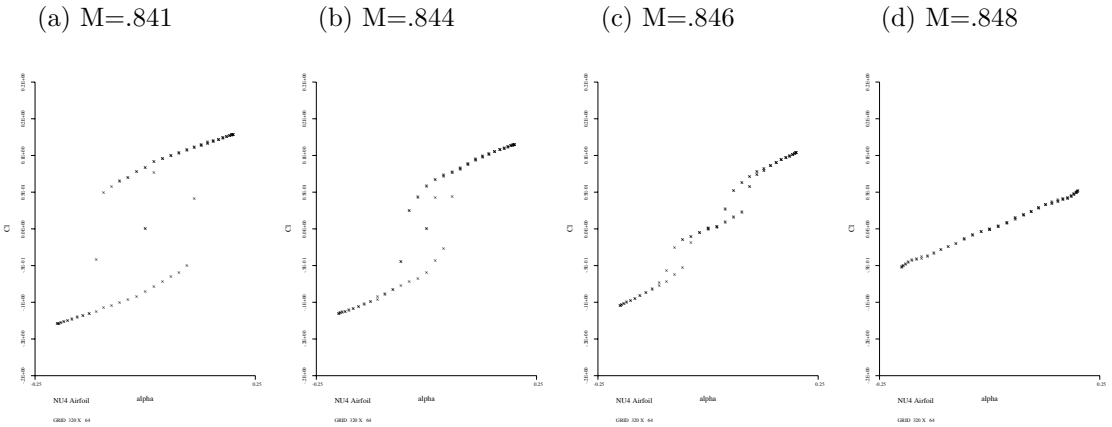

Figure 7. CL-α sweeps for NU4 airfoil at decreasing Mach numbers.

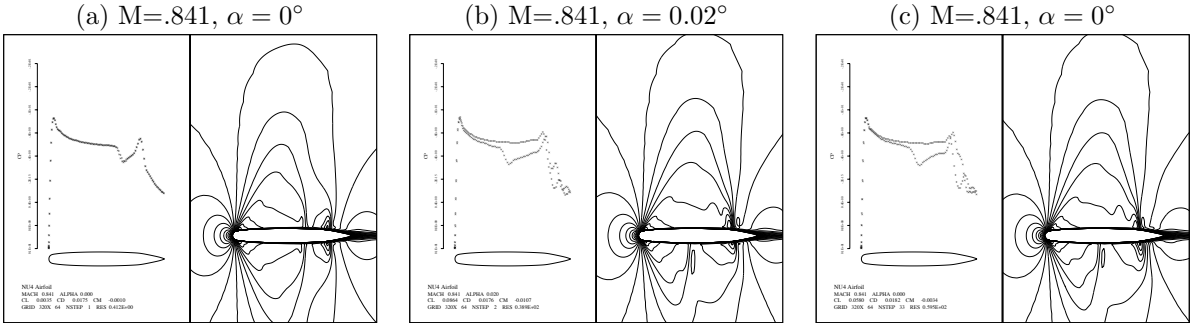

Figure 8. Cp distributions for NU4 airfoil at M.841. (a) Flow solution at zero angle of attack. (b) Flow solution at 0.02 degree angle of attack (c) Flow solution at zero angle of attack, following an initial perturbation to 0.02 degree angle of attack.

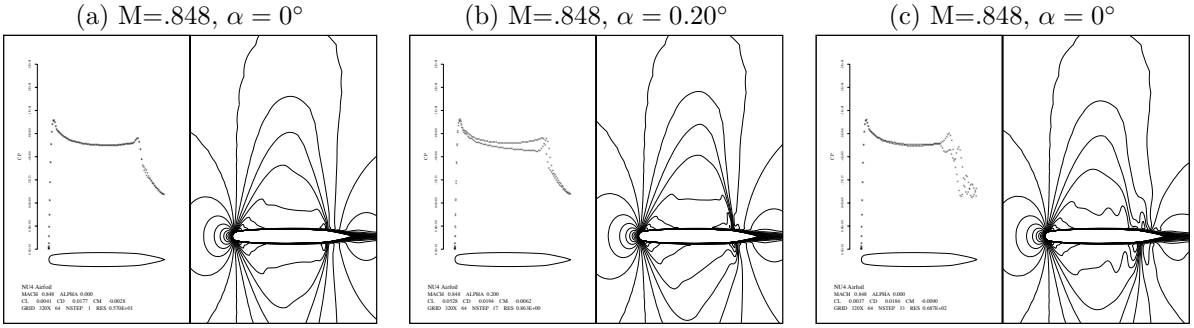

Figure 9. Cp distributions for NU4 airfoil at M.848. (a) Flow solution at zero angle of attack. (b) Flow solution at 0.2 degree angle of attack (c) Flow solution at zero angle of attack, following an initial perturbation to 0.2 degree angle of attack.

small change in α caused two closely spaced shocks to coalesce into one single shock. The newly formed flow supporting the single shock is stable even after the original α is restored. At M=.848, the airfoil admits only a single shock on each airfoil surface. Without interaction of multiple shocks, the transonic flows remain unique.

III. Non-unique Transonic Flows: RANS Solution vs Euler Solution

In this section, comparisons are made between the unsteady RANS solution and the Euler solution for the same airfoils at the same Mach numbers that admit non-unique solutions in the previous study using Euler solver. Due to the presence of boundary layers, especially near the trailing edges, the exact location, strength, and resolution of the shocks tend to be different, but the global flow characteristics remain quite similar.

III.A. JB1 Airfoil M.827

The unsteady RANS and Euler results for the JB1 airfoil at M.827 are shown in Figure 10, 11, and 12. Both solvers produce three types of solution branches, as are shown in the CL-α sweeps in Figure 10. The CL-α sweep from the RANS calculations is not as smooth and clean as the Euler calculations. This is a consequence of the unsteady nature of the flow simulation, as expected when shocks interact with the boundary layers close to the airfoil trailing edge, as can be seen in the pressure contours in Figure 12. Multiple branches can clearly be identified in Figure 10 (a). In addition to the P-, Z-, and N-branches that are typical of the Euler solution, an additional Z-branch with a steeper gradient can also be identified.

(a) Unsteady RANS Solution

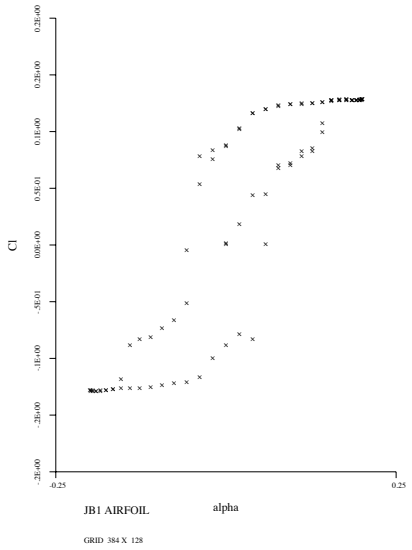

(b) Steady Euler Solution

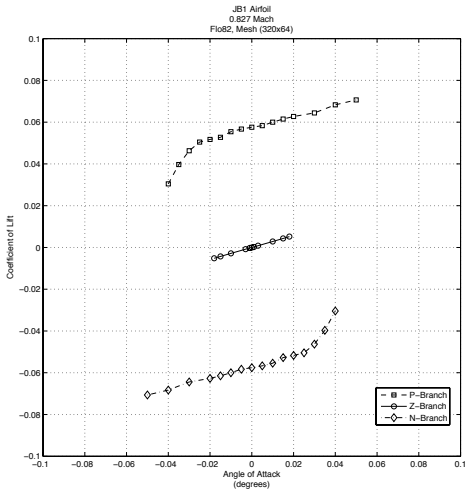

Figure 10. Plots of CL-α sweep for flows over the JB1 airfoil at M.827, showing the presence of the positive, negative, and zero branches.

At zero angle of attack, a symmetrical and an asymmetrical solutions are admitted by both solvers, and the corresponding flow solutions are plotted in Figure 13 and 14. Comparing the RANS solution with the Euler solution, the presence of the boundary layer in the RANS solution reduces the effective curvature of the airfoil near the trailing edge, with the consequence that the shock strength is reduced, and the shock location slightly different. However, the number of the shocks on each surface and their patterns remain very similar.

(a) RANS solution, M=.827, $\alpha = 0°$

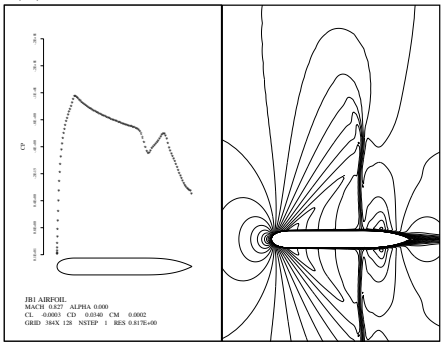

(b) Euler solution, M=.827, $\alpha = 0°$

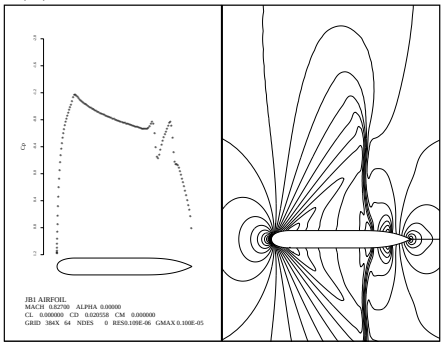

Figure 11. Pressure contours showing the symmetric flow solutions of JB1 airfoil at $\alpha = 0°$, M=.827

(a) RANS solution, M=.827, $\alpha = 0°$

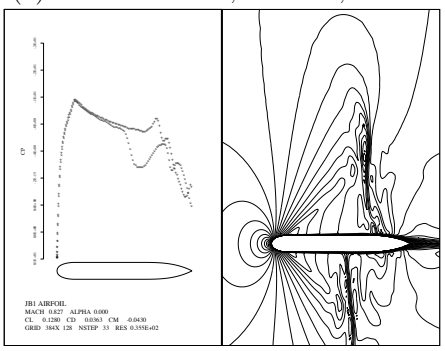

(b) Euler solution, M=.827, $\alpha = 0°$

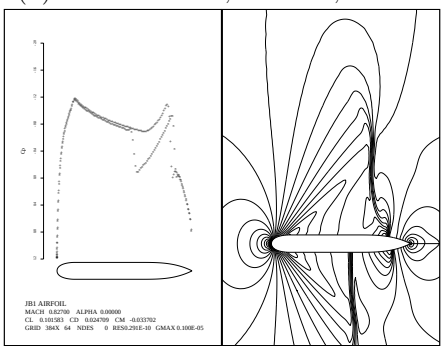

Figure 12. Pressure contours showing the asymmetric flow solutions of JB1 airfoil at $\alpha = 0°$, M=.827. The asymmetric solutions are obtained by first perturbing the airfoil to a positive attitude, before restoring it back to zero angle of attack.

III.B. JF1 Airfoil M.835

The unsteady RANS and Euler results for the JF1 airfoil at M.835 are shown in Figure 13, 14, and 15. At this Mach number, the Euler solution shows three distinctive branches. The unsteady RANS solution, on the other hand, does not show such distinctive solution branches at this Mach number, though the branches become more distinctive at other Mach numbers. Examining the pressure contours, it can be observed that for this airfoil at M.835, the shock is located very close to the trailing edge. Because the boundary layer is thick, the flows tend to be unsteady, the flow solution and shock location are not as distinctive as the corresponding Euler solution. This is reflected in the plot of CL - α sweep.

(a) Unsteady RANS Solution (b) Steady Euler Solution

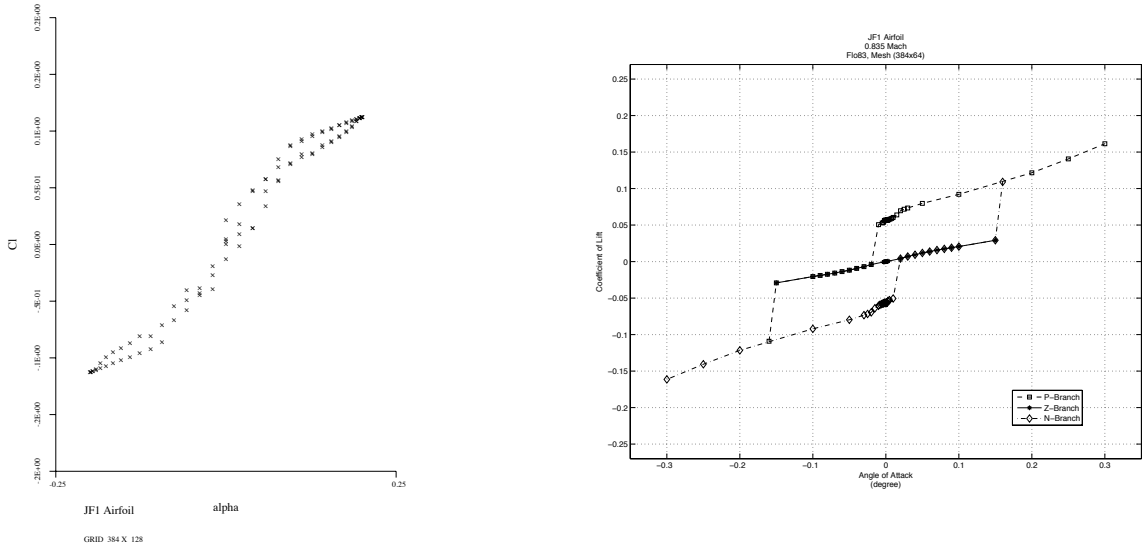

Figure 13. Plots of CL-α sweep for flows over the JF1 airfoil at M.835.

Figure 14 also shows that symmetrical flow at zero angle of attack is not a very stable condition, as a result of the proximity of shock to the trailing edge boundary layer. A more stable solution is one with one shock on one side, and two shocks on the other side, as shown in Figure 15.

(a) RANS solution, M=.835, $\alpha = 0°$ (b) Euler solution, M=.835, $\alpha = 0°$

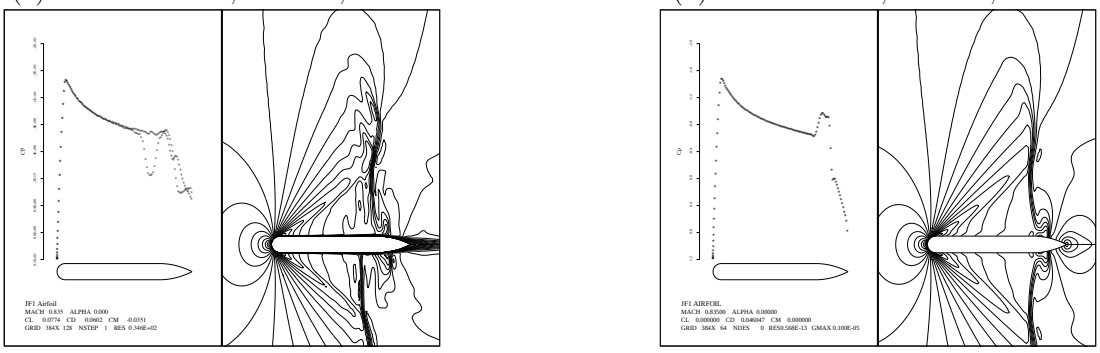

Figure 14. Pressure contours showing the flow solutions of JF1 airfoil at $\alpha = 0°$, M=.835

III.C. NU4 Airfoil M.840

The unsteady RANS and Euler results for the NU4 airfoil at M.840 are shown in Figure 16, 17, and 18. The unsteady RANS solution shows only the P- and N-branches at this Mach number, while the Euler solution shows all three. The NU4 airfoil exhibits three branches in other Mach numbers. Examples can be seen in

(a) RANS solution, M=.835, $\alpha = 0°$ (b) Euler solution, M=.835, $\alpha = 0°$

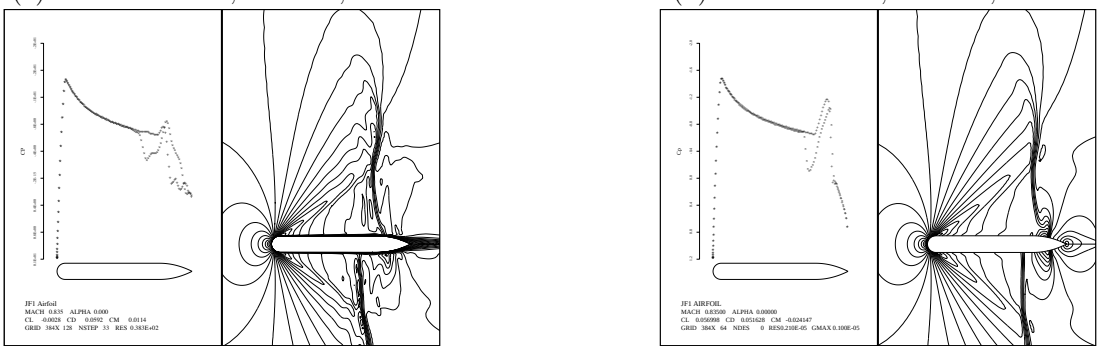

Figure 15. Pressure contours showing the asymmetric flow solutions of JF1 airfoil at $\alpha = 0°$, M=.835. The asymmetric solutions are obtained by first perturbing the airfoil to a positive attitude, before restoring it back to zero angle of attack.

Figure 4 and Figure 7. At this Mach number, the NU4 airfoil does not have a distinctive Z-branch because the shock is located close to the trailing edge. As a result of the interaction between the shock and the boundary layer, the symmetrical solution is less stable than the asymmetrical solution.

(a) Unsteady RANS Solution (b) Steady Euler Solution

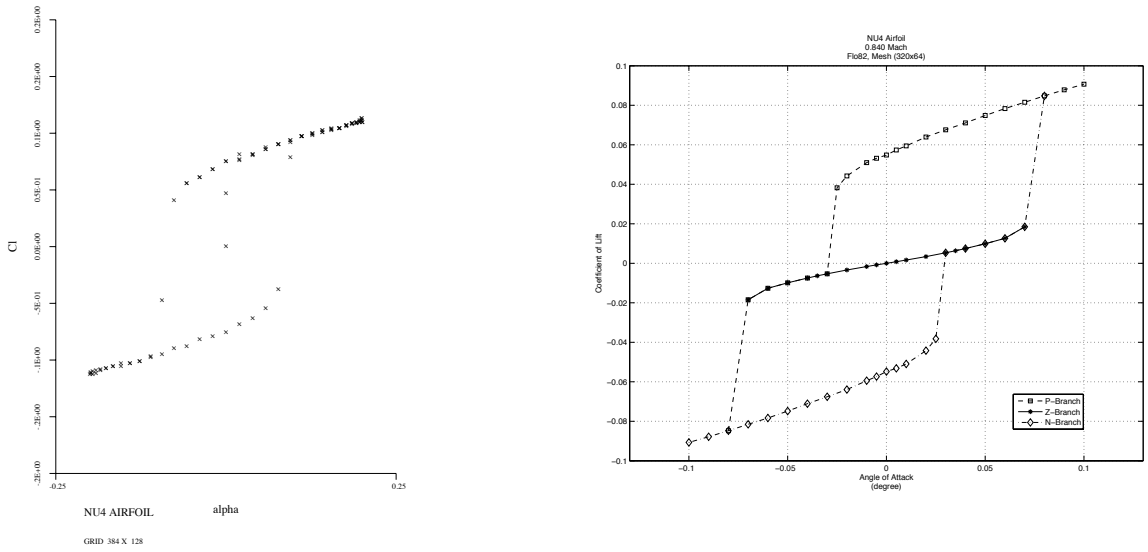

Figure 16. Plots of CL-α sweep for flows over the NU4 airfoil at M.840.

III.D. JC6 Airfoil M.847

The unsteady RANS and Euler results for the JC6 airfoil at M.847 are shown in Figure 19, 20, and 21. Again, the JC6 does not have a very distinctive Z-branch. The interaction between the shocks and the boundary layer makes it difficult to maintain a symmetrical solution, as shown in Figure 20. The solution after initial perturbation, on the other hand, looks very similar to the Euler solution, as shown in Figure 21. In general, the trailing edge stagnation pressure from the RANS calculation does not recover to the leading edge stagnation pressure as well as the Euler solution does, as expected.

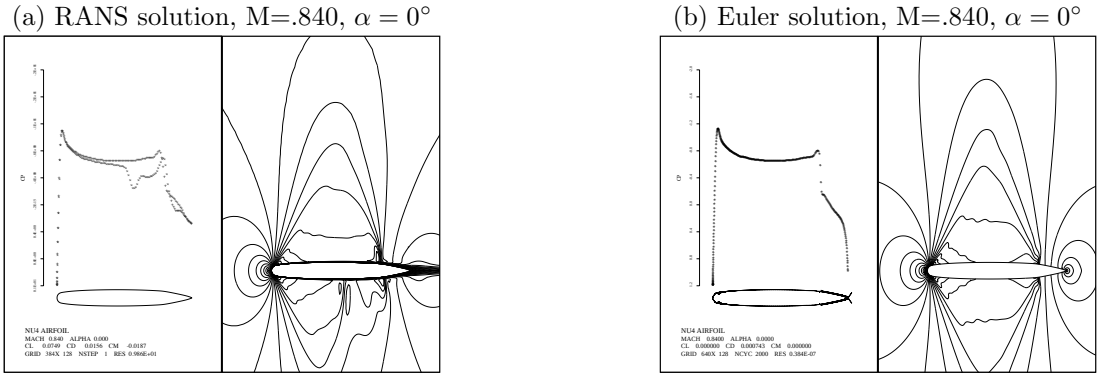

Figure 17. Pressure contours showing the flow solutions of NU4 airfoil at $\alpha = 0°$, M=.840

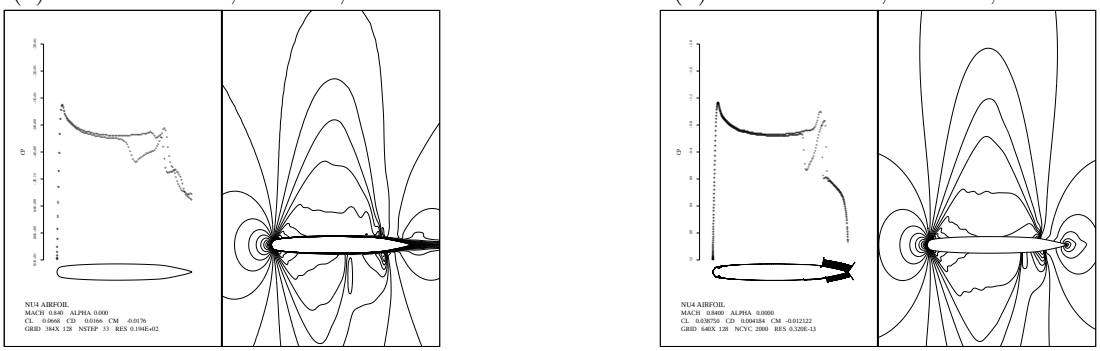

Figure 18. Pressure contours showing the asymmetric flow solutions of NU4 airfoil at $\alpha = 0°$, M=.840. The asymmetric solutions are obtained by first perturbing the airfoil to a positive attitude, before restoring it back to zero angle of attack.

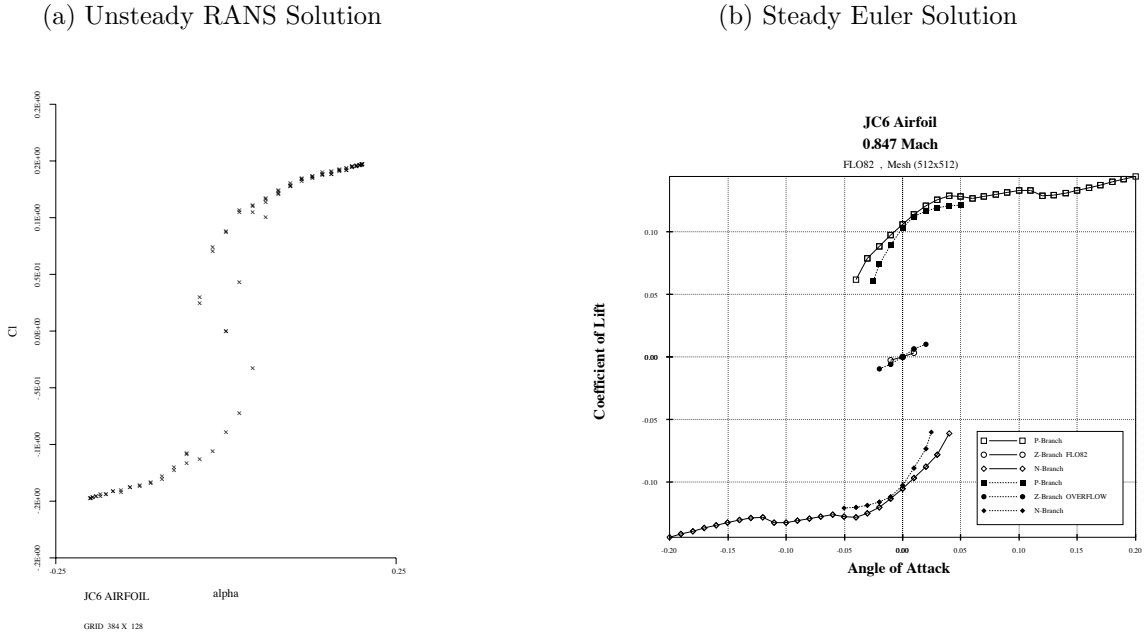

Figure 19. Plots of CL-α sweep for flows over the JC6 airfoil at M.847.

(a) RANS solution, M=.847, $\alpha = 0°$

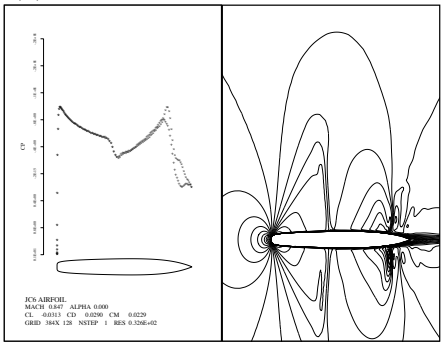

(b) Euler solution, M=.847, $\alpha = 0°$

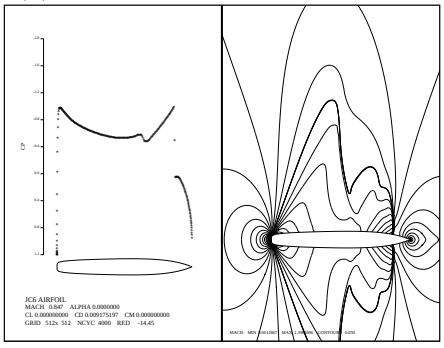

Figure 20. Pressure contours showing the flow solutions of JC6 airfoil at $\alpha = 0°$, M=.847

(a) RANS solution, M=.847, $\alpha = 0°$

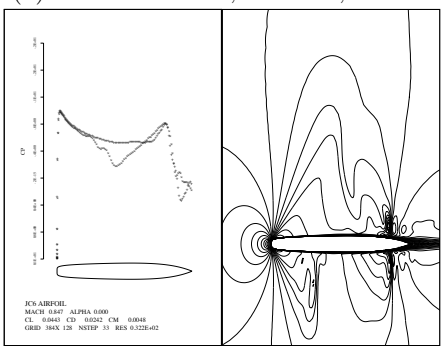

(b) Euler solution, M=.847, $\alpha = 0°$

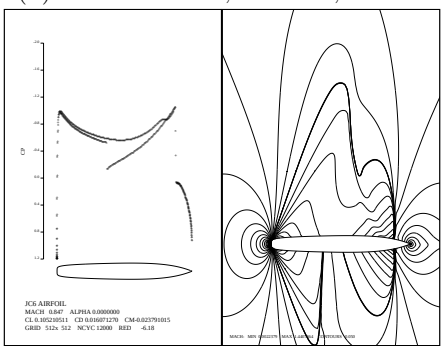

Figure 21. Pressure contours showing the asymmetric flow solutions of JC6 airfoil at $\alpha = 0°$, M=.847. The asymmetric solutions are obtained by first perturbing the airfoil to a positive attitude, before restoring it back to zero angle of attack.

IV. Discussion

Experience from shape optimization of transonic airfoils shows that a nearly shock free airfoil tends to operate near a very singular point. When flow is slightly perturbed from this singular point, a double shock will tend to form on the airfoil surface when perturbed one way, and a single shock will form when perturbed in the other way. The concept is illustrated in the sketch in Figure 22, where the dashed line indicates a shock free condition.

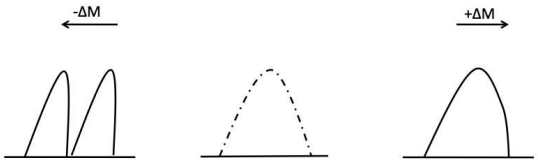

Figure 22. Illustration of plausible flow behaviors following a perturbation from a shock-free condition.

For a symmetric airfoil in critical transonic flow, a small disturbance in angle of attack increases the local Mach number on one side of the airfoil, and decreases the local Mach number on the other side. As a result, a double shock can form on the side with decreasing flow speed, and a single shock can form on the side with increasing flow speed. The pressure jump across the double shock tends to increase the pressure, leading to lift generation following the perturbation. This increase in lift generates a circulation around the airfoil in such a way that the initial local speed perturbation is further reinforced. This leads to a stabilizing mechanism. As a result, even when the initial perturbation is removed, i.e. the angle of attack is restored to the initial attitude of zero, the flow does not restore to the original pattern due to the stabilizing mechanism. The mechanism is illustrated in Figure 23. The negative of this can also occur, yielding a complementary state of negative lift or circulation.

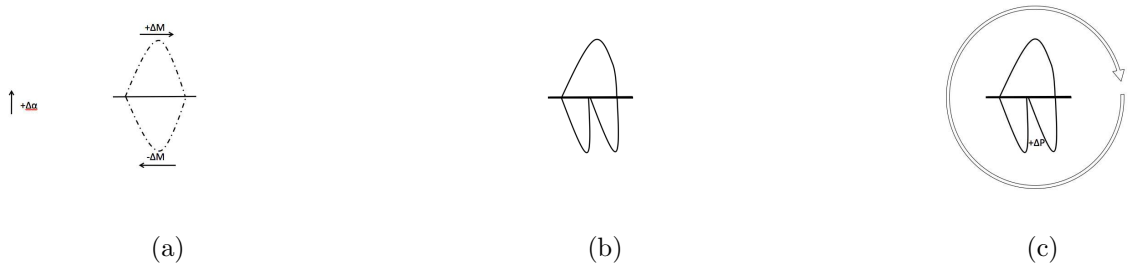

Figure 23. Illustration of the stabilizing effect of circulation on transonic flow solution.

V. Conclusion

Non-unique transonic flows were previously found to exist for steady Euler solutions. In this study, non-unique transonic flows for unsteady RANS solutions are also found to exist. Comparison between the RANS and the Euler solutions, it is observed that the Euler solution is able to capture the global flow characteristics quite well, despite its simplification. Time accurate simulations, on the other hand, indicate that the symmetric solutions (i.e. Z-branch solutions) are not as stable as the steady state solver indicates. The stability depends on the strength and location of the shock wave, and the state of the boundary layer. The non-unique solutions appear when weak double shocks appear on the airfoil. The existence of non-

unique depends on the relative separation of the shocks, for a given perturbation. An initial perturbation that is significant enough to cause the shocks to interact and coalesce is more likely to lead to the creation of non-unique solutions.

References

[1]J. Steinhoff, and A. Jameson, *Multiple solution of the transonic potential flow equations*, AIAA J. 20(11), 15211525 (1982)

[2]M.D. Salas, R.E. Melnik, and A. Jameson, *A comparative study of the non-uniqueness problem of the potential equation*, AIAA Paper 83-1888, (1983)

[3]A. Jameson, *Airfoil admitting non-unique solutions to the Euler equations*, AIAA Paper 91-1625 (1991)

[4]M.M. Hafez and W.H. Guo, *Nonuniqueness of transonic ows*, Acta Mech. 138, 177184 (1999a)

[5]M.M. Hafez and W.H. Guo, *Some anomalies of numerical simulation of shock waves*, Part I: inviscid ows. Comput. Fluids 28(45), 701719 (1999b)

[6]M.M. Hafez and W.H. Guo, *Some anomalies of numerical simulation of shock waves. Part II: effect of articial and real viscosity*, Comput. Fluids 28(45), 721739 (1999c)

[7]A.G. Kuzmin and A.V. Ivanova, *The structural instability of transonic flow associated with amalgamation/splitting of supersonic regions*, Theoret. Comput. Fluid Dynamics (2004) 18:335-344

[8]A.G. Kuzmin, *Instability and bifurcation of transonic flow over airfoils*, AIAA Paper, 2004

[9]A.V. Ivanova and A.G. Kuzmin, *Non-uniqueness of the transonic flow past an airfoil*, Fluid Dynamics, Vol. 39, No.4, pp.642-648, (2004)

[10]A.G. Kuzmin, *Bifurcation of transonic flow over a flattened airfoil*, Frontiers of Computational Fluid Dynamics, World Scientific Publishing Company LTD, (2006)

[11]Kuzmin, *Structural instability of transonic flow over an airfoil*, Journal of Engineering Physics and Thermophysics, Vol. 77, No.5, pp.1022-1026, (2004)

[12]J. C. Vassberg, N. A. Harrison, D. L. Roman and A. Jameson, *Systematic Study on the Impact of Dimensionality for a Two-Dimensional Aerodynamic Optimization Model Problem*, 29^{th} AIAA Applied Aerodynamics Conference, Honolulu, HI, June, 2011

[13]A. Jameson, W. Schmidt, and E. Turkel, *Numerical Solutions of the Euler Equations by Finite Volume Methods Using Runge-Kutta Time-Stepping Schemes*, AIAA Paper 81-1259, AIAA 14th Fluid and Plasma Dynamic Conference, Palo Alto, (1981)

[14]A. Jameson, *.Time dependent calculations using multigrid, with applications to unsteady flows past airfoils and wings.*, AIAA Paper 91-1596, AIAA 10th Computational Fluid Dynamic Conference, Hawaii (1991).

[15]A. Jameson, J. Vassberg, and K. Ou, *Further Studies of Airfoils Supporting Non-unique Solutions in Transonic Flow*, AIAA Journal, DOI: 10.2514/1.J051713, Vol. 50, No. 12, pp. 2865-2881, December 2012.